NASA CONTRACTOR
REPORT

NASA CR-129040

CHARACTERIZATIONS OF FOUR SPECIMENS PROCESSED AS A PART OF THE M553 SPHERE FORMING EXPERIMENT PERFORMED DURING THE SKYLAB 1 and 2 FLIGHT

By J.L. Hubbard, J.W. Johnson, J.L. Brown
Georgia Institute of Technology
Atlanta, Georgia 30332

December 1973

Prepared for

NASA-GEORGE C. MARSHALL SPACE FLIGHT CENTER
Marshall Space Flight Center, Alabama 35812

TECHNICAL REPORT STANDARD TITLE PAGE

1. REPORT NO.	2. GOVERNMENT ACCESSION NO.	3. RECIPIENT'S CATALOG NO.
NASA CR-129040		

4. TITLE AND SUBTITLE	5. REPORT DATE
Characterizations of Four Specimens Processed as a Part of the M553 Sphere Forming Experiment Performed During the Skylab 1/2 Flight	December 1973
	6. PERFORMING ORGANIZATION CODE

7. AUTHOR(S)	8. PERFORMING ORGANIZATION REPORT #
J. L. Hubbard, J.W. Johnson, J.L. Brown	

9. PERFORMING ORGANIZATION NAME AND ADDRESS	10. WORK UNIT NO.
Georgia Institute of Technology Atlanta, Georgia 30332	11. CONTRACT OR GRANT NO. NAS 8-28735
	13. TYPE OF REPORT & PERIOD COVERED Contractor Report Summary
12. SPONSORING AGENCY NAME AND ADDRESS National Aeronautics and Space Administration Washington, D.C. 20546	14. SPONSORING AGENCY CODE

15. SUPPLEMENTARY NOTES

16. ABSTRACT

Four specimens identified as SL-1.3, SL-1.8, SL-1.9 and SL-2.5 were submitted to the Engineering Experiment Station at Georgia Tech on July 17, 1973, for metallurgical characterization. These specimens had been processed in the M512 Facility as a part of the M553 Sphere Forming Experiment performed during the Skylab 1/2 flight. Three of these specimens, SL-1.3, SL-1.8, and SL-2.5 were designed to be melted completely by the electron beam and detach themselves from their support posts and resolidify while floating free in the near zero gravity and vacuum environment of space. Specimens SL-1.3 and SL-1.8 were completely melted, but it is believed they did not leave their posts before solidifying. Specimen SL-2.5 was only partially melted. Specimen SL-1.9 was to be completely melted and retained on a large sting which was accomplished as planned.

The nominal composition of the four specimens was as follows:

SL-1.3	Ni 12% Sn
SL-1.8	Ni 30% Cu
SL-1.9	Pure Ni
SL-2.5	Pure Ni

These four specimens have been examined according to the Phase B Characterization Plan established by this laboratory. The results are discussed and compared with similar characterization analyses run on ground base specimens.

17. KEY WORDS	18. DISTRIBUTION STATEMENT
	Unclassified - Unlimited

19. SECURITY CLASSIF. (of this report)	20. SECURITY CLASSIF. (of this page)	21. NO. OF PAGES	22. PRICE
Unclassified	Unclassified	47	NTIS

TABLE OF CONTENTS

LIST OF FIGURES

LIST OF FIGURES (Continued)

LIST OF FIGURES (Continued)

LIST OF FIGURES (Concluded)

INTRODUCTION

Four specimens identified as SL-1.3, SL-1.8, SL-1.9 and SL-2.5 were submitted to the Engineering Experiment Station at Georgia Tech on July 17, 1973 for metallurgical characterization. These specimens had been processed in the M512 Facility as a part of the M553 Sphere Forming Experiment performed during the Skylab 1/2 flight. Three of these specimens, SL-1.3, SL-1.8, and SL-2.5 were designed to be melted completely by the electron beam and detach themselves from their support posts and resolidify while floating free in the near zero gravity and vacuum environment of space. Specimens SL-1.3 and SL-1.8 were completely melted, but it is believed they did not leave their posts before solidifying. Specimen SL-2.5 was only partially melted. Specimen SL-1.9 was to be completely melted and retained on a large sting which was accomplished as planned.

The nominal composition of the four specimens was as follows:

SL-1.3	Ni 12% Sn
SL-1.8	Ni 30% Cu
SL-1.9	Pure Ni
SL-2.5	Pure Ni

These four specimens have been examined according to the Phase E Characterization Plan established by this laboratory. The results are discussed and compared with similar characterization analyses run on ground base specimens.

CHARACTERIZATION PROCEDURES

Visual Observations

Each of the four Skylab specimens was carefully observed under a stereo microscope. Precise notes were taken concerning the shape of the specimens, the degree of melting, the presence of surface contaminants, and the position and nature of any unusual features.

Optical Macroscopy

Optical macrographs were taken of each of the specimens from six different orthogonal directions. These micrographs were taken on a Bausch & Lomb "L" camera using a 48 millimeter Micro Tessar lens. A few stereomacrographs were recorded using a 6 degree tilt between the left and right views.

Radiography

Radiographs of each of the specimens were made using a Baltograph II x-ray generator operating at 135 KV with a tungsten target to reveal the position and size of any voids present.

Scanning Electron Microscopy

A Cambridge Stereoscan Mark II-A equipped with a Kevex-ray-Northern Scientific energy dispersive x-ray analyzer and a Quantimet 720 image analyzing computer was used to examine the Skylab specimens. Each of the specimens was mounted in a special stub designed to hold spheres and placed in the scanning electron microscope for observations. Micrographs of the surfaces were taken using the following systematic technique. Some great circle on the surface of each sample was chosen on which was exemplified all of the different surface features characteristic of that particular specimen. Low magnification micrographs (25X) were made in the SEM along that great circle at intervals of 30 degrees. Higher magnification micrographs were made in each area to show the typical surface structures, any unusual features, and any surface contaminants. The location of the area from which the higher magnification micrographs were made was marked on the low magnification shots. A few stereomicrographs were recorded using a 10 degree difference between the left and right views. Energy dispersive x-ray analysis for elemental content was performed on general areas of each specimen as well as on unusual features and contaminant particles.

Electron Probe Microanalysis

An Acton MS64 electron probe microanalyzer was used for a more accurate analysis of the elemental content. Analyses were run in general areas of each specimen as well as on any unusual features found either through the optics of the microprobe or previously in the scanning electron microscope.

X-ray Spectroscopy

Quantitative elemental analysis of each sample on a gross scale was made using a Siemens Crystalloflex IV x-ray fluorescence unit operating at 40 KV with a tungsten target.

Section Preparations

Each of the specimens was positioned on a carbon block and held in place with sealing wax so that a cut could be made through a plane whose perimeter included all of the various structures seen on the specimen surface. Sectioning was done on a Micromatic Precision Wafering Machine using a 10 mil thick silicon carbide wheel. After sectioning, one half of each of the specimens was mounted in a casting resin so that the cut face could be prepared for examination. The specimens were mechanically polished using a series of abrasive papers and wet polishing wheels through a 0.3 micron alumina and electropolished using a Disa-Electropolisher. Electropolishing was accomplished on the pure Ni and the Ni-Ag and Ni-Sn alloys using the A2 electrolyte solution containing:

Perchloric acid	7[illegible] x 10^{-6} m^3
Distilled water	120 x 10^{-6} m^3
Methyl alcohol	700 x 10^{-6} m^3
Butyl cellosolve	100 x 10^{-6} m^3

Electropolishing of the Ni-Cu alloy was accomplished using the E2 electrolyte solution containing:

Ferric chloride	5 x 10^{-6} kg
Concentrated HCl	2 x 10^{-6} m^3
Methyl alcohol	99 x 10^{-6} m^3

Emission Spectroscopy

A small amount of material was removed from the center of the unmounted half of each specimen by drilling a small shallow hole in the center of each cut face. The shavings thus produced were placed in a cavity of a carbon spectrographic rod and burned to completion in an Applied Research Laboratories 1.5 meter grating emission spectrograph. The near ultraviolet radiation was recorded on Kodak Spectrum Analysis No. 1 Film and analyzed on an Applied Research Laboratories comparator.

Electron Probe Microanalysis of Sections

Each of the polished sections was analyzed in the electron microprobe. Analyses were made of general areas of the sections, across grains, in and along dendritic features, in eutectics and in any unusual features seen. Standards supplied by Dr. Theo Kattamis of the University of Connecticut were used to obtain quantitative data from these analyses.

Optical Examination of Specimen Sections

Optical macrographs of each of the polished and etched sections were taken using a Bausch and Lomb "L" camera and a 48 millimeter lens. Micrographs were taken to demonstrate all of the various microstructures present on each section using a Leitz Metallux optical microscope.

Scanning Electron Microscopy of Sections

Each of the specimen sections was removed from its mount and placed in the scanning electron microscope for observation. Micrographs were taken of both typical and unusual features and some nondispersive x-ray analyses were performed.

INDIVIDUAL CHARACTERIZATIONS

Specimen SL-1.3

Results of Characterization Analyses. Specimen SL-1.3 is a nickel-tin alloy which was cast rather than machined into the original specimen shape due to the brittle nature of this material. The specimen was well rounded except for a flat area which shall henceforth be referred to as the bottom. One side of the specimen was rough in appearance showing a coarse dendritic structure with a large amount of porosity. The opposite side was relatively smooth. Figure 1 is a side view of this specimen with the rough side on the left, the smooth side on the right and the flat area on the bottom. Protrusions from the flat area as seen on the bottom left of Figure 1 appear to be areas where liquid metal touched and adhered to some surface, probably the alumina support post, and remained during solidification. Solidification appears to have started from these protrusions since columnar dendrites growing directionally from these areas are seen on the surface. Farther up the side the dendrites become more equiaxed and random with porosity increasing on the upper portion of this side. Near the top as shown in Figure 2 is an area of small circular dendritic features which begins and ends abruptly. A very similar area was seen on the Ni-Sn ground base Specimen 2-7. The two dark lines seen in the bottom right of Figure 1 run approximately half way around the specimen and are believed to be features of the original cast structure.

The only contamination seen visually on this specimen was a small black spot shown in the upper center of Figure 1 and the lower center of Figure 2.

Radiography revealed the porosity in the upper portion of the rough side of this specimen and revealed no large voids present.

Figure 3 is a scanning electron micrograph of the columnar dendrites on the rough side of Specimen SL-1.3. The equiaxed dendrites and associated porosity found farther up this rough side are shown in Figure 4. The abrupt change from the equiaxed dendrites to the small circular dendrites at the top is shown in Figures 5 and 6. The structure of the smooth side of the specimen, shown in Figure 7 resembles the as cast structure seen on the ground base specimens. Figure 8 is a low magnification micrograph taken normal to the bottom of the specimen showing the two lines mentioned earlier which appear to be part of the original cast structure. Energy dispersive x-ray analysis from different areas of the sample surface did not indicate any differences in

composition. Analysis of a few of the charged particles seen on some of the figures did not show any detectable elements indicating that these particles consist of lighter elements and are organic in nature. They probably contaminated the surface in handling after the completion of the Skylab experiment.

Analysis of the surface in the electron microprobe revealed contaminants of Cu, Fe, and a trace of W in various areas. Some areas analyzed showed a high Sn content.

X-ray fluorescence analysis of the entire sample shows the Sn concentration to be 9.4 percent.

Emission spectrographic analysis of some of the material from the center of the specimen gave the following trace elemental content:

Si	20 PPM
Fe	10 PPM
Cu	2 PPM

Electropolishing of this sample revealed enough of the microstructure, as seen through the optics of the electron microprobe, to allow for good selective quantitative analysis of various features. The microstructure, which will be shown later in optical and scanning electron micrographs of the etched section, was revealed in two forms. On about one half of the cross section, that half bounded by the smooth surface of the specimen, the microstructure showed grains surrounded by a thin line of a second phase material. Dispersed throughout this structure was another phase in the form of "lakes" which were also surrounded by a thin line of apparently the same second phase material. This structure is shown in Figure 10. Microprobe analysis from within the grains in this structure gave varying amounts of Sn concentration from a high of 9.5 percent to a low of 7.3 percent in those grains analyzed. The Sn concentration in the second phase material surrounding the grains averaged 16.8 percent. Within a number of "lakes" analyzed the Sn concentration varied from a high of 35.5 percent to a low of 28.6 percent. On the opposite half of the cross section the microstructure was dendritic with a darker appearing material similar to that of the "lakes" captured within the dendritic structures. The grains formed by each dendrite were surrounded by a thin line of the second phase material. This structure is shown in Figures 11 and 12. The Sn concentration in the darker or "lakes" features analyzed in this structure ranged from 26.8 percent to 22.5 percent. The Sn concentration across dendrite arms varied from 4.6 percent in the center of an arm to 12.5 percent between arms. Microprobe analysis of general areas

of the cross section showed a variation in the Sn concentration with no definite pattern noticable. However, the Sn concentration in the area showing grain structure varied from 14.6 percent to 11.2 percent while in the dendritic area it varied from 12.5 percent to 8.9 percent. In the very porous area near the surface of the specimen the elemental concentrations were found to be Ni-92.1 percent, Sn-5.3 percent and O-2.6 percent.

Figure 9 is an optical macrograph of the polished and etched cross section of Specimen SL-1.3. Optical and scanning electron micrographs of the microstructure are shown in Figures 10 through 13. The microstructure in the area of the cross section bounded by the smooth side of the sample seen on the left in Figure 9 is shown in Figure 10. The dendritic structure seen in the lower right of Figure 9 is shown in Figures 11 and 12. The transition region between these two microstructures is shown in Figure 13. Figure 14 shows the structure in a porous region of the specimen section.

Summary. From the evidence presented by the characterization analyses it is believed that only a portion of Specimen SL-1.3 was actually melted and that it did not leave its support post during resolidification. Solidification began with the growth of columnar dendrites from the contact areas. This columnar dendritic region is relatively small in this specimen. Solidification proceeded with the formation of equiaxed dendrites. The cap area was probably surface nucleated and solidified some time before final solidification. The external porosity in the equiaxed dendritic region near the cap is due to solidification shrinkage.

The specimen apparently had a considerable amount of absorbed oxygen in its cast state which expanded in the molten metal in the vacuum environment giving rise to a very porous resolidified structure internally. There was also a considerable loss of Sn in the melted and resolidified material due to evaporation.

Specimen SL-1.8

Results of Characterization Analysis. Specimen SL-1.8 is a nickel-copper alloy which is nearly spherical in shape except for a very flat smooth region on which the specimen rested during solidification. Figure 15 is a profile view of this specimen showing the flat contact region on the right. From the flat region to almost half way up the specimen, the surface is a smooth tight structure of columnar dendrites. Above this region there is a band in which the structure becomes increasingly rougher and more porous until it ends abruptly in a smooth nonporous cap which covers the top one-third or more of the specimen. This cap is made up of small circular dendrites. The surface structure of this specimen is very similar to that of the nickel-copper ground base Specimen 2-10.

A gold stain was observed on one side of the specimen.

Radiography revealed no large voids present in the specimen.

Figure 16 is a low power scanning electron micrograph showing the three different surface structures on this specimen. The flat area is shown in profile at the top of this micrograph. Figure 17 is a high magnification micrograph of the columnar dendrites which have grown directionally away from the flat region as shown in Figure 16. The abrupt change from the porous band of equiaxed dendrites to the cap area of fine circular dendrites is shown in Figure 18. Figure 19 shows the structure of the circular dendrites in this cap region. There appears to be a large amount of porosity beneath the cap region, at least at its edge as demonstrated in Figure 20.

The surface of the sample contained a large number of contaminating particles. The following elements were found in varying amounts on those particles analyzed using energy dispersive x-ray analysis:

Al, Si, S, Cl, K, Ca, Ag and Ti

A number of Al_2O_3 particles were identified on the surface using electron microprobe analysis. Quantitative analysis from randomly selected spots on the surface showed a large variation in the amount of copper present from a high of 27.6 percent to a low of 6.1 percent. No pattern of Cu content versus surface position or surface features was found.

X-ray spectroscopy analysis shows the Cu concentration in this sample as a whole to be 23.3 percent. This analysis, of course, is representative more of the surface of the sample than of the interior.

Emission spectrographic analysis of some of the material from the center of the specimen gave the following trace elemental content:

Si	20 PPM
Fe	20 PPM
Ag	20 PPM
Pb	5 PPM
Ca	6 PPM

Electron microprobe analysis from selected areas on the specimen cross section showed the copper concentration near the flat side and in the center to be almost equal and averaged 28.4 percent. In the region near the cap, however, the average dropped to 25.6 percent.

Figure 21 is an optical macrograph of the polished and etched cross section of Specimen SL-1.8. Optical and scanning electron micrographs of the microstructures are shown in Figures 22 through 28. Figure 22 shows the microstructure in the cap region of the specimen. The porosity and microstructure associated with the external porous band are shown in Figures 23 and 24. The random equiaxed dendrites in the center of the section are shown in Figures 25 and 26 and the columnar dendrites near the flat region are shown in Figures 27 and 28.

Summary. This specimen was apparently completely melted by the electron beam and either floated free in space but collided with some smooth flat surface before solidifying, or more probably, remained adhered to its support post during solidification. The specimen had a smooth flat area on the surface due to this adherence during solidification.

Solidification began from the flat contact region with the growth of columnar dendrites which extend from the flat region through about one third of the specimen. This columnar dendritic region is followed by a region of randomly oriented equiaxed dendrites. A large amount of porosity is associated with these dendrites on the surface of the specimens due to solidification shrinkage. The portion of the sample surface directly opposite the flat region is covered with a continuous cap made up of fine circular dendrites believed to have been formed by surface nucleation.

The nominal composition of this alloy before processing in space was 70 percent Ni, 30 percent Cu. Analysis has shown that a considerable amount

of copper was lost by evaporation during processing. It was further found that less copper was present in the cap area, particularly at the surface, than was in the remainder of the specimen. The microchemistry of the dendrites and interdendritic regions, however, is in agreement with the phase diagram for this alloy.

There was some contamination on the surface of this specimen. Some of this was attributable to particles from the support posts but the remainder is unexplained.

Specimen SL-1.9

Results of Characterization Analyses. Specimen SL-1.9 is a pure nickel material which was purposely retained on its sting after melting. The specimen is egg shaped and glossy with smooth dendritic features on the surface. The area near the sting position is curved and appears to have melted, at least internally, but had retained some of the machine markings of the original specimen surface. At the top of the specimen, opposite the sting area, is a slight protrusion. In and around this protrusion is a much finer dendritic structure. A gold discoloration was seen on one side of the specimen. Figure 29 is a profile view of this specimen showing a small portion of the sting on the right and the protrusion previously mentioned on the left.

Radiography revealed two voids present near the bottom of the specimen as shown in Figure 30. These voids are approximately 0.65mm and 0.2mm in diameter.

Figure 31 is a scanning electron micrograph of the surface of Specimen SL-1.9 near the sting. The surface features nearer the top of the specimen are shown in Figures 32 and 33. The amount of contamination seen in Figure 33 was typical of the entire surface of this specimen. The protrusion on the top of the specimen and the finer dendritic structure associated with it are shown in Figure 34. The interface at the edge of this protrusion is shown at higher magnification in Figures 35 and 36.

Energy dispersive x-ray analysis of contaminants seen on the specimen surface gave varying amounts of the following elements:

Al, Si, S, Cl, K, Ca and Ag

One particle found embedded in a void gave high counts of Cr, Mn and Fe.

The gold discoloration on the side of the specimen was analyzed in the electron microprobe to be carbon. No additional elements than those found by energy dispersive analysis were found by microprobe analysis.

Emission spectrographic analysis of some of the material from the center of the specimen gave the following trace elemental content:

Si	20 PPM
Fe	5 PPM
Al	10 PPM
Cr	10 PPM

Electron microprobe analysis of the polished cross section revealed a small amount of oxygen in a few spots. No other elements were found.

Figure 37 is a macrograph of the polished and etched section of Specimen SL-1.9. The microstructure is shown in Figures 38 and 39. Figure 38 shows the structure near the sting portion of the section. Figure 39 was taken at the boundary of the protrusion near the top of the specimen. The pits seen on these figures are etch pits and seem to form only in resolidified areas as will be shown in Specimen SL-2.5. The stain seen on either side of the protrusion in Figures 37 and 39 was always present after etching although the section was polished and etched a number of times. This reaction remains unexplained at this time.

Summary. Specimen SL-1.9 was apparently completely melted and purposely retained on its sting during resolidification. Solidification was initiated from the sting with the growth of large columnar grains. The grains nearer the top of the specimen are smaller and more equiaxed. A protrusion exists on top of the specimen which may have been produced by surface nucleation and growth in this area before final solidification. The voids in this sample were probably a result of absorbed or reabsorbed gases expanding within the molten metal.

The surface of the sample was badly contaminated and at least part of this was due to handling after completion of this experiment.

Specimen SL-2.5

Results of Characterization Analyses. Specimen SL-2.5 is a pure nickel material which was not completely melted by the electron beam. The resolidified surface was glossy in appearance with dendritic features and a large number of pores present. At the top of the specimen, diametrically opposed to the sting, was a protrusion very similar to the one seen on Specimen SL-1.9. This protrusion had fine "tree" like dendrites and circular dendrites both of which were more evident near its periphery. Figure 40 is a profile view of this specimen showing the unmelted portion in the upper right and the protrusion on the far left.

Radiography revealed no voids present in this specimen.

Figure 41 is a scanning electron micrograph of the resolidified surface of Specimen SL-2.5 near the sting side showing some of the pores present. More dendritic like ridges are evident near the top of the specimen as shown in Figure 42. Figure 43 shows the protrusion at the top of the specimen. The dendritic structures seen near the periphery of this protrusion are shown in Figures 44 and 45. Figure 44 shows the "tree" like dendrites while Figure 45 shows the circular dendritic features. Near the top of the specimen, next to the unmelted portion, there are many pores in the surface as shown in Figure 46. The unmelted portion seen in the lower right of this figure shows no machine markings indicating some surface melting did occur in this area. The resolidified surface next to the unmelted portion at the bottom of the specimen exhibits peaks as shown in Figure 47.

Energy dispersive x-ray analysis of contaminants seen on the specimen surface gave either no results, indicating possible organics, or gave varying amounts of the following elements:

Al, Si, Cl, and Ca

Microprobe analysis of the surface revealed a thin layer of Cu on one side of the specimen. Also, Al_2O_3 particles were found frequently all over the resolidified portion and one spot was found which showed Fe and Cr.

Emission spectrographic analysis of some of the material from the center of the specimen gave the following trace elemental content:

Si	20 PPM
Fe	5 PPM
Cu	10 PPM
Al	10 PPM
Ca	20 PPM
Cr	20 PPM

Electron microprobe analysis of the polished cross section gave no significant findings.

Figure 48 is a macrograph of the polished and etched cross section of Specimen SL-2.5

The microstructure is shown in Figures 49 through 51. Figure 49 shows the microstructure in the unmelted portion of the specimen. The grains are larger in this area than in the original material indicating recrystallization has occurred. Figure 50 shows the boundary between the resolidified and unmelted regions. This figure also demonstrates the existence of the etch pits only in the resolidified region. Figure 51 shows the structure in the resolidified region near the top of the specimen.

Summary. Specimen SL-2.5 was not completely melted in the electron beam but the unmelted portion recrystallized. The resolidified grain size, however, was larger than the recrystallized grains. A protrusion exists on top of the specimen similar to the one seen on Specimen SL-1.9. This protrusion probably formed as a result of surface nucleation and growth before final solidification. No voids were formed in the specimen but the surface had a large number of pores present.

The surface of the specimen was contaminated with particles from the support post, from evaporated material from other specimens, and from handling after the experiment was complete.

RESULTS AND CONCLUSIONS

The external appearances of the four Skylab specimens characterized by this laboratory are very similar to those of the ground test specimens of the same alloys. One exception, perhaps, is the protrusion seen on the top of the pure nickel specimens. All of the specimens, both flight and ground base, were in contact with some other surface or with unmelted material during solidification. Therefore, since the thermal gradients during cooling were similar on both experiments, the similarities of the specimens is not unexpected. The specimens processed in space apparently remained molten for a longer period of time than did the ground base specimens. The result was a greater loss in alloying elements by evaporation in the Skylab specimens.

Some differences in microsegregation or microchemistry may be seen in the Skylab versus ground tests but the statistics are not sufficient to make any definitive statements. These differences might also be due to a longer molten state period than to zero gravity effects.

Future experimentation in materials processing in space such as the M553 experiment must require more preliminary scientific input into the procedure and design of apparatus. More research is needed in the design of support posts to which the materials to be tested will not adhere and in proper systems for the deployment of the molten specimen. More usable data gathering techniques must be employed during the experiment such as fast frame movie cameras monitoring for the duration of each specimen test, voice data on observed results, temperature monitoring, etc. Specimen handling should also be performed under clean room conditions. In order to obtain the most in scientific knowledge of zero gravity effects on materials processing the number of unknown variables must be brought to a minimum.

Figure 1. Profile view of Specimen SL-1.3 (10X).

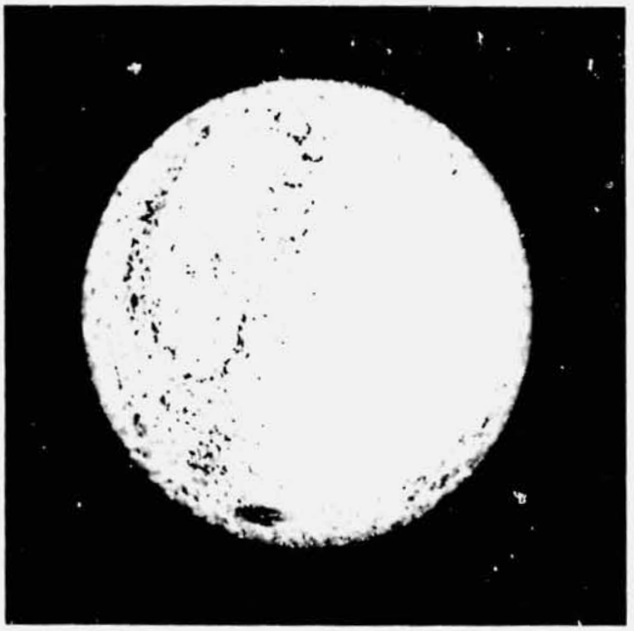

Figure 2. Top view of Specimen SL-1.3 (10X).

Figure 3. Scanning electron micrograph of the columnar dendrites on the surface of Specimen SL-1.3 (100X).

Figure 4. Scanning electron micrograph of the equiaxed dendrites and porosity on the surface of Specimen SL-1.3 (100X).

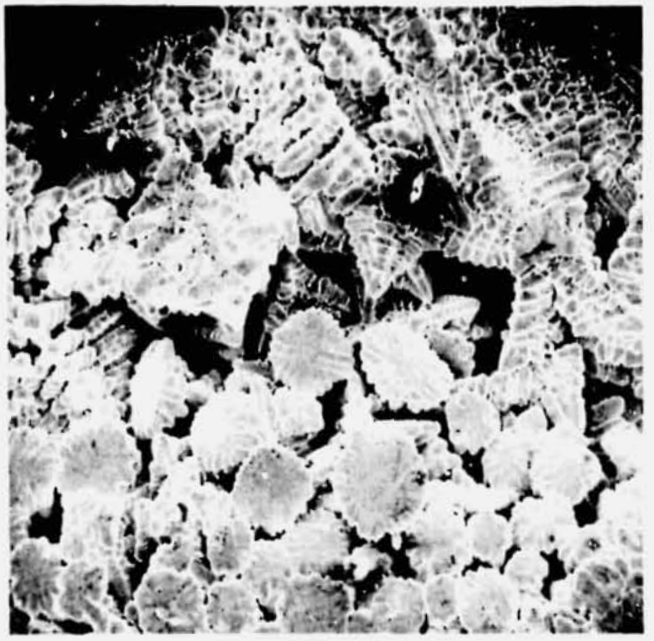

Figure 5. Scanning electron micrograph of the abrupt change from equiaxed to small circular dendrites on Specimen SL-1.3 (100X).

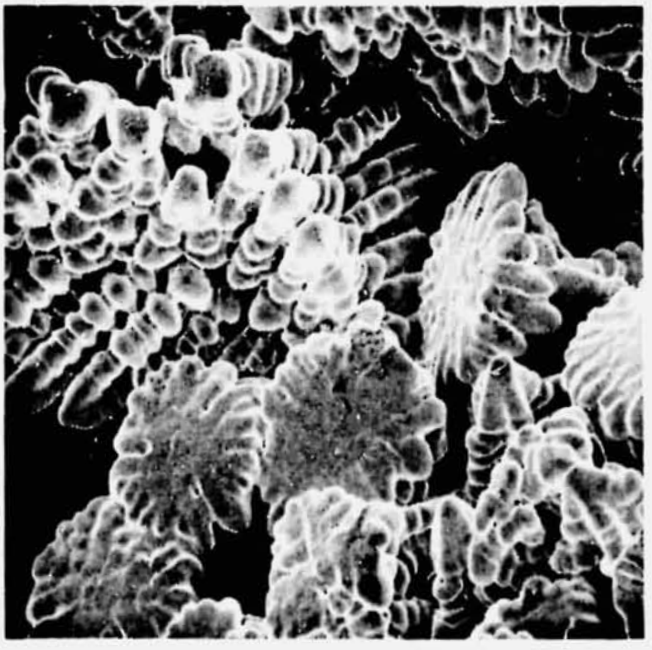

Figure 6. Scanning electron micrograph of the abrupt change from equiaxed to small circular dendrites on Specimen SL-1.3 (250X).

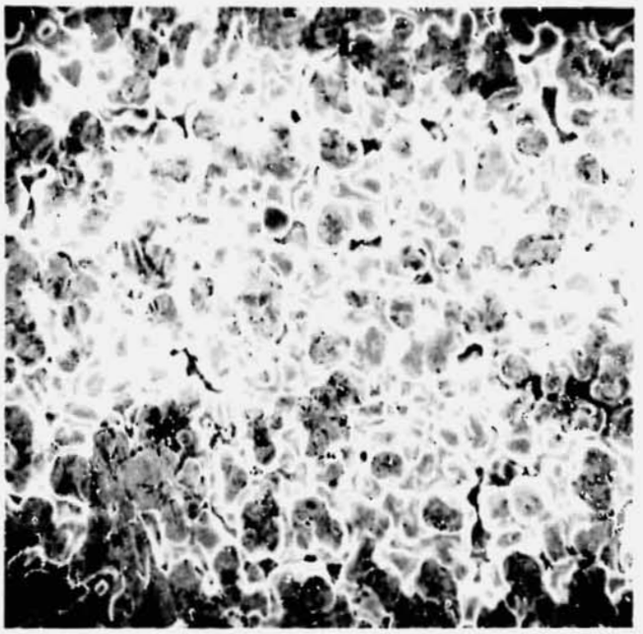

Figure 7. Scanning electron micrograph of the smooth side of Specimen SL-1.3 (250X).

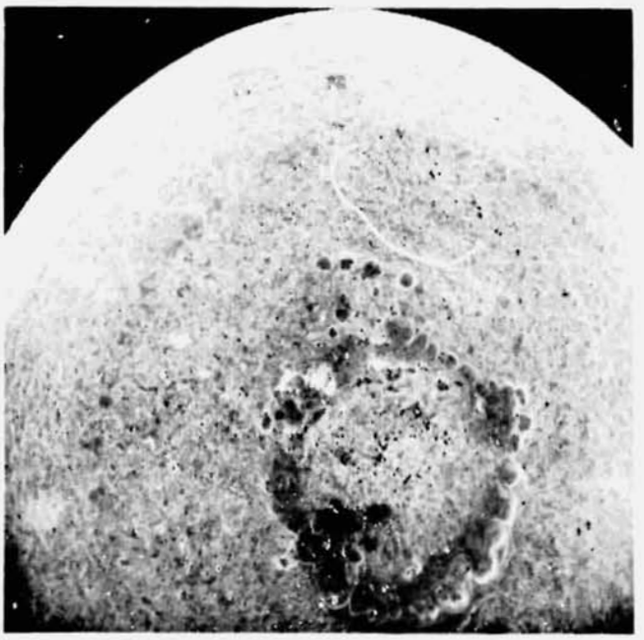

Figure 8. Scanning electron micrograph taken normal to the bottom of Specimen SL-1.3 (25X).

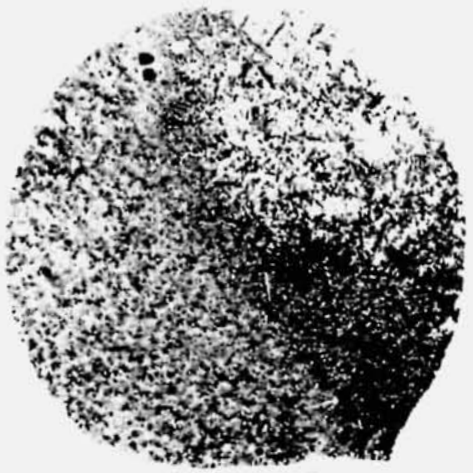

Figure 9. Polished and etched cross section of Specimen SL-1.3 (10X).

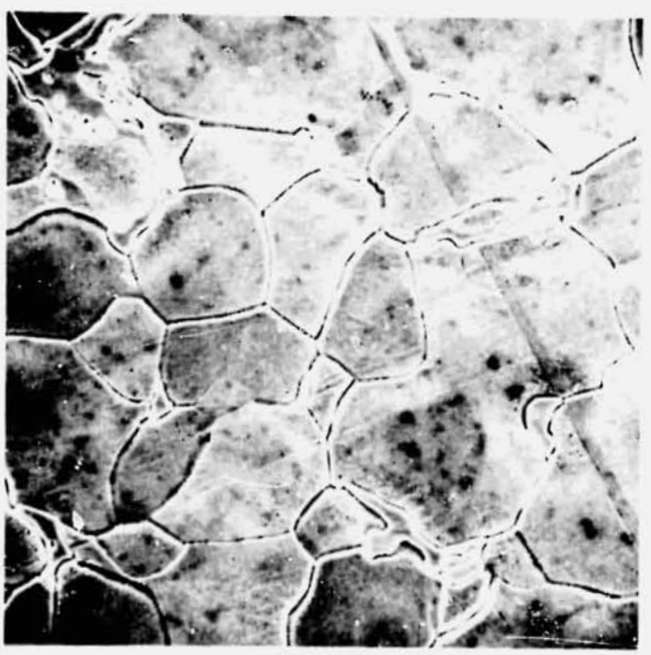

Figure 10. Scanning electron micrograph of the microstructure in the cross section near the smooth surface of Specimen SL-1.3 (1000X).

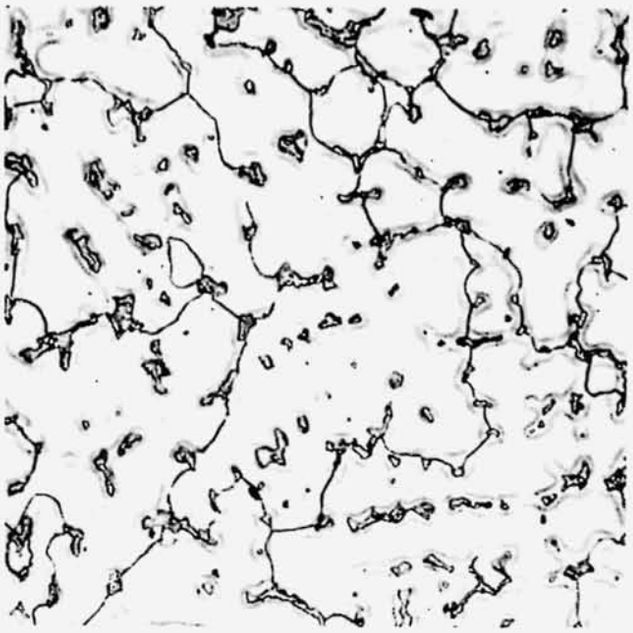

Figure 11. Optical micrograph of the dendritic structure in the cross section of Specimen SL-1.3 (250X).

Figure 12. Scanning electron micrograph of the dendritic structure in the cross section of Specimen SL-1.3 (250X).

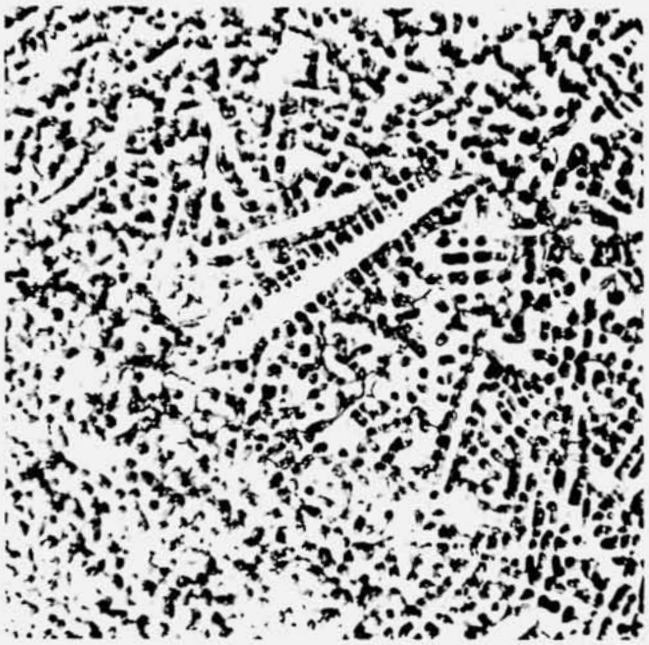

Figure 13. Optical micrograph of the transition region between grains and dendrites in the cross section of Specimen SL-1.3 (100X).

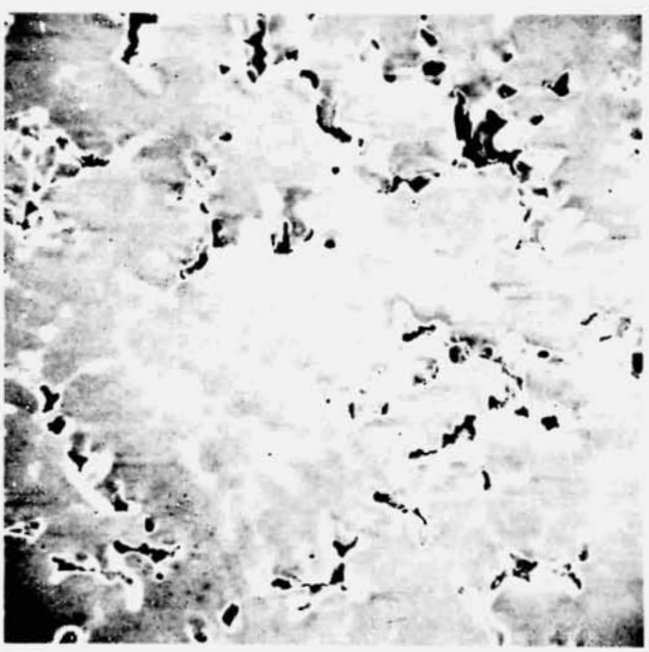

Figure 14. Scanning electron micrograph of the porous region of the cross section of Specimen SL-1.3 (250X).

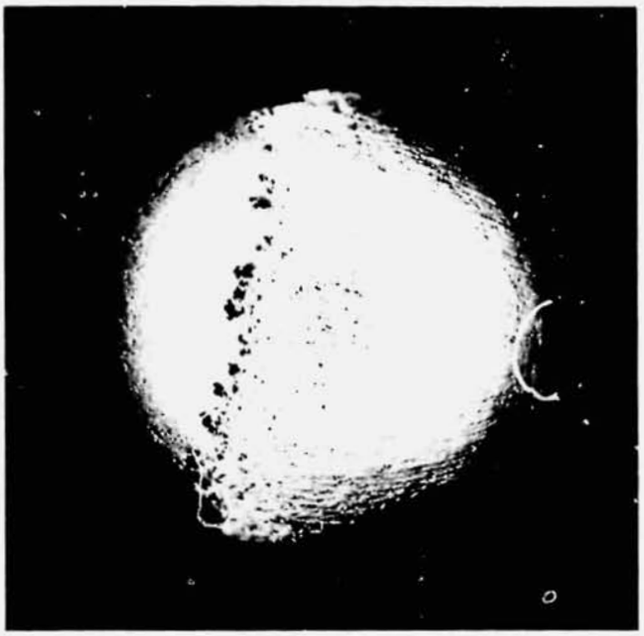

Figure 15. Profile view of Specimen SL-1.8 (10X).

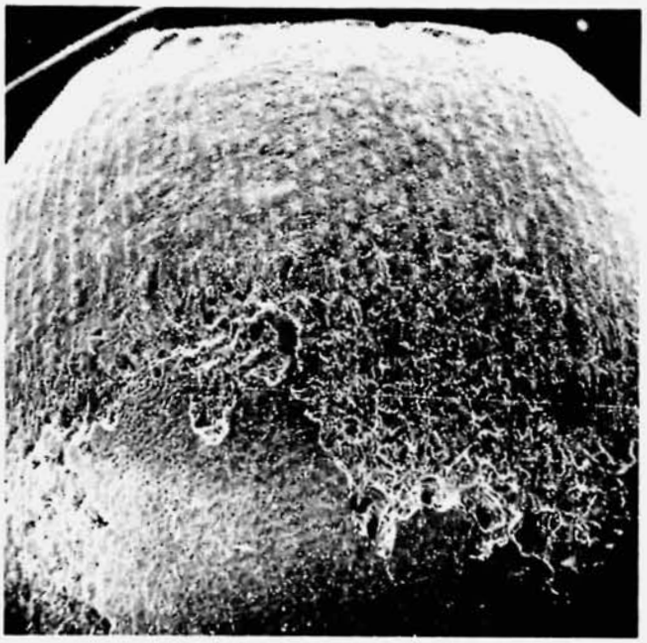

Figure 16. Scanning electron micrograph of the three surface structures on Specimen SL-1.8 (25X).

Figure 17. Scanning electron micrograph of the columnar dendrites on the surface of Specimen SL-1.8 (250X).

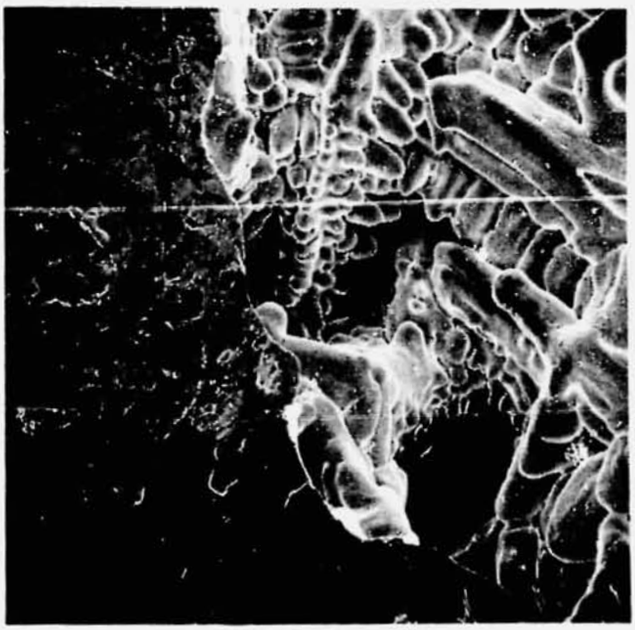

Figure 18. Scanning electron micrograph of the abrupt change from equiaxed dendrites to the cap region on Specimen SL-1.8 (250X).

Figure 19. Scanning electron micrograph of the circular dendrites in the cap region of Specimen SL-1.8 (250X).

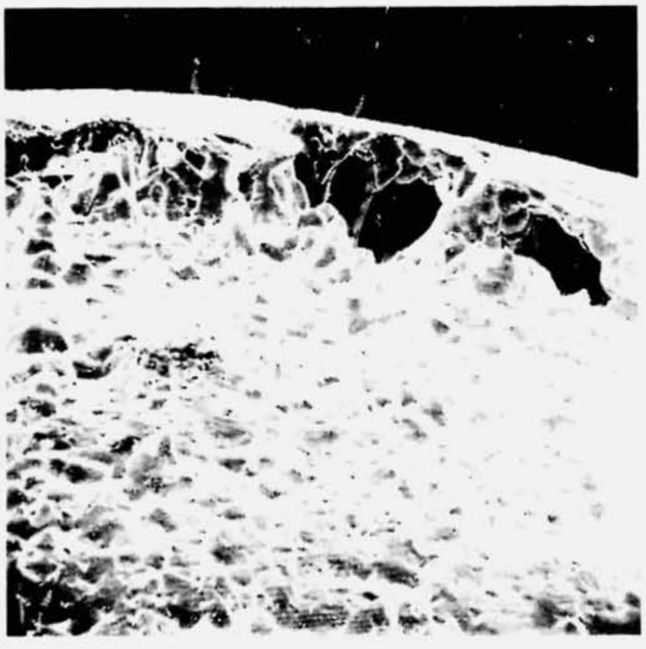

Figure 20. Scanning electron micrograph of the edge of the cap region of Specimen SL-1.8 (100X).

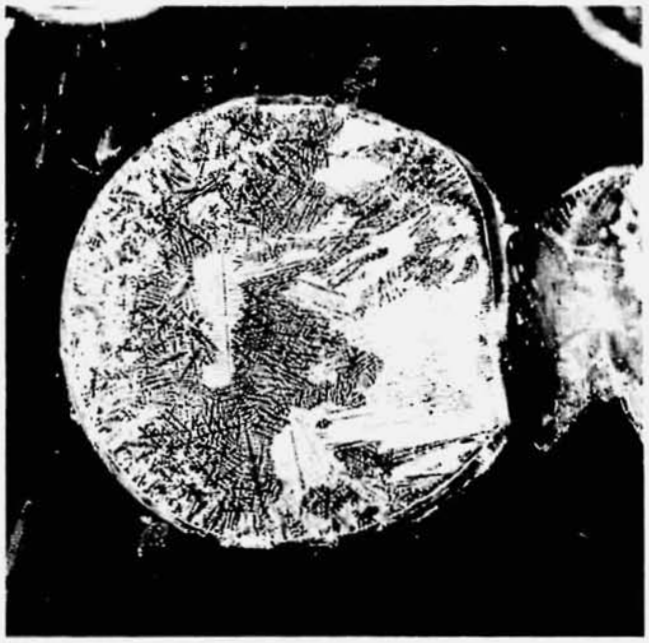

Figure 21. Optical macrograph of the polished and etched cross section of Specimen SL-1.8 (10X).

Figure 22. Scanning electron micrograph of the microstructure near the cap region in the cross section of Specimen SL-1.8 (100X).

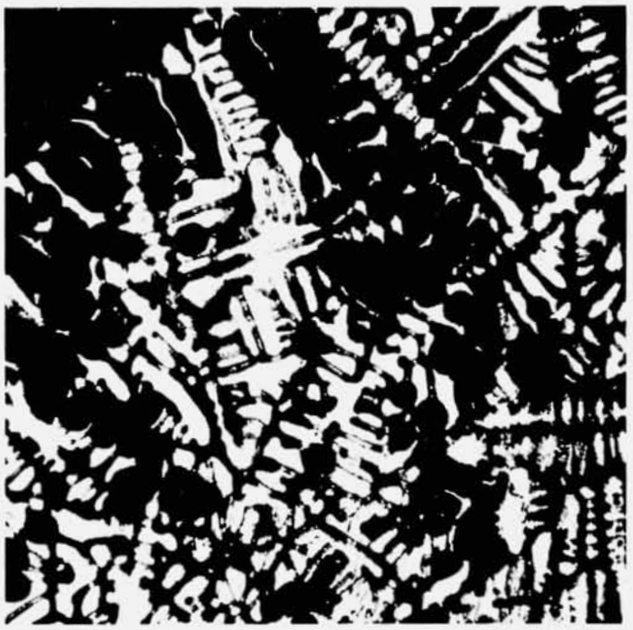

Figure 23. Optical micrograph of the microstructure near the porous band in the cross section of Specimen SL-1.8 (100X).

Figure 24. Scanning electron micrograph of the microstructure near the porous band in the cross section of Specimen SL-1.8 (100X).

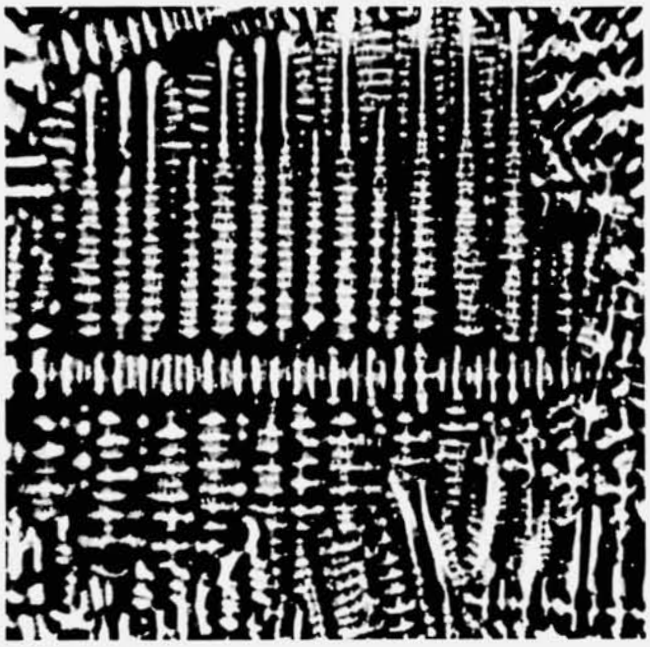

Figure 25. Optical micrograph of the microstructure near the center of the cross section of Specimen SL-1.8 (100X).

Figure 26. Scanning electron micrograph of the microstructure near the center of the cross section of Specimen SL-1.8 (250X).

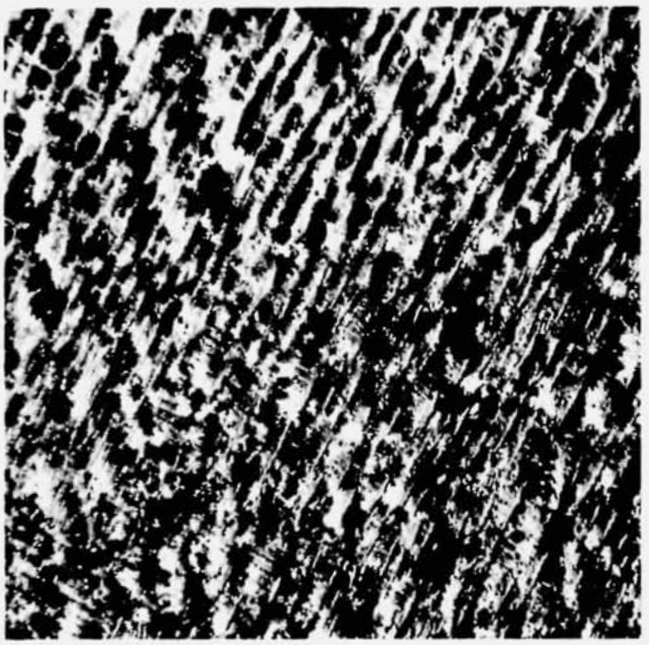

Figure 27. Optical micrograph of the columnar dendritic structure in the cross section of Specimen SL-1.8 (100X).

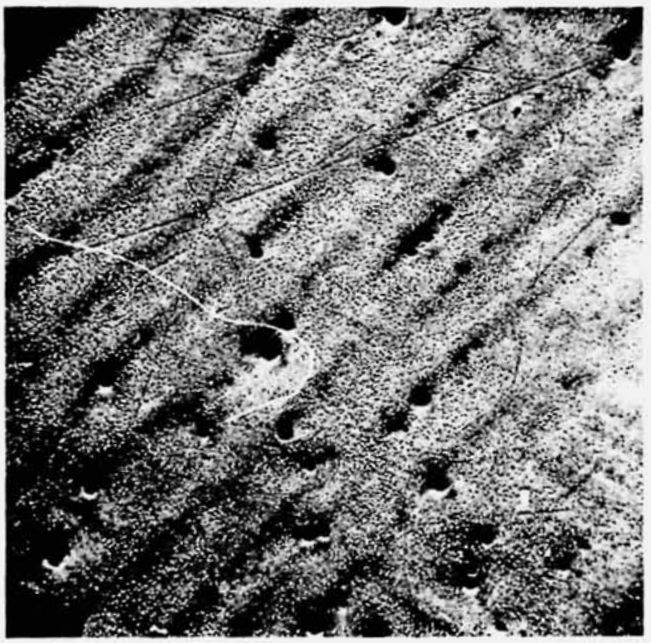

Figure 28. Scanning electron micrograph of the columnar dendritic structure in the cross section of Specimen SL-1.8 (500X).

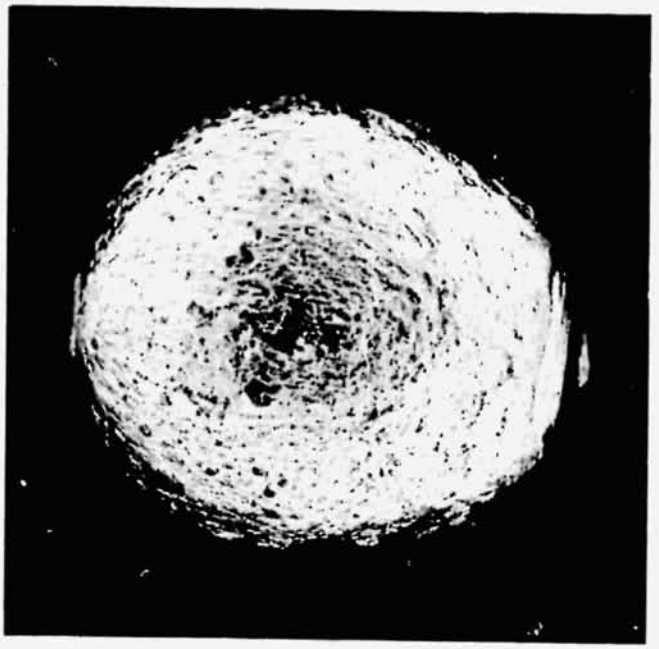

Figure 29. Profile view of Specimen SL-1.9 (10X).

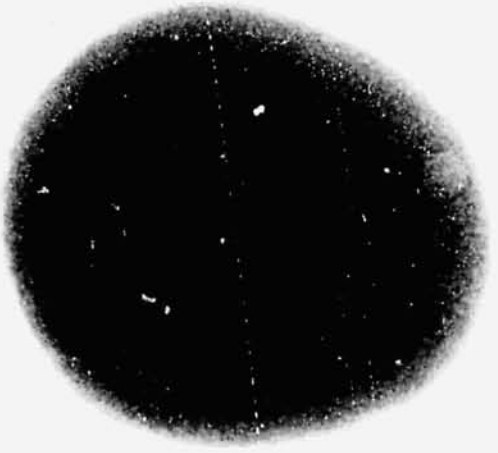

Figure 30. Radiograph of Specimen SL-1.9 (10X).

Figure 31. Scanning electron micrograph of the surface of Specimen SL-1.9 near the sting (100X).

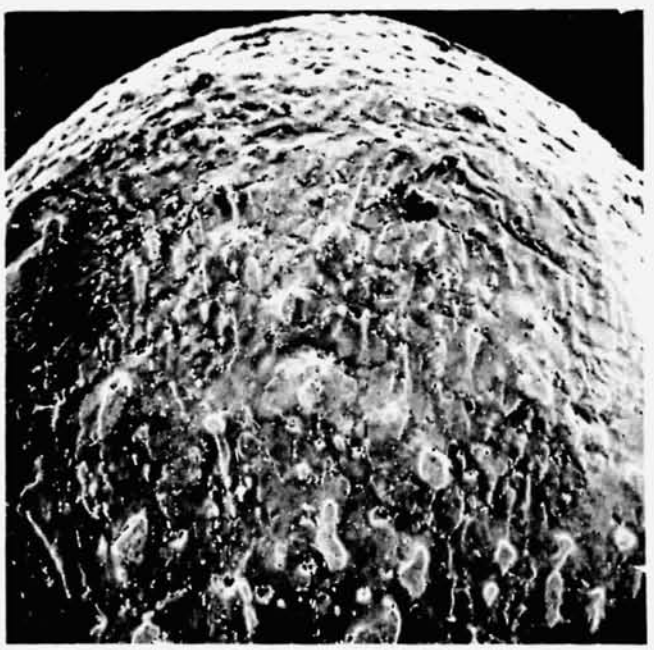

Figure 32. Scanning electron micrograph of the surface of Specimen SL-1.9 near the top (25X).

Figure 33. Scanning electron micrograph of the surface of Specimen SL-1.9 near the top (250X).

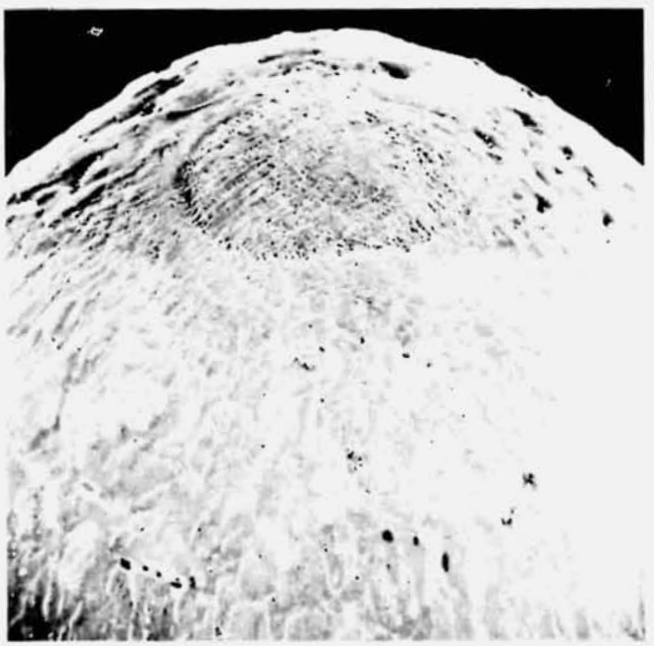

Figure 34. Scanning electron micrograph of the top protrusion on Specimen SL-1.9 (25X).

Figure 35. Scanning electron micrograph of the edge of the top protrusion on Specimen SL-1 9 (100X).

Figure 36. Scanning electron micrograph of the edge of the top protrusion on Specimen SL-1.9 (100X).

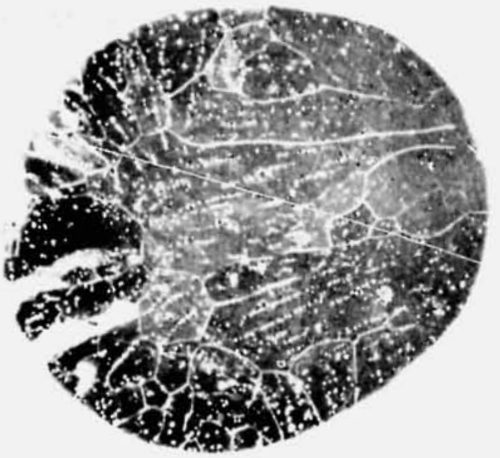

Figure 37. Polished and etched cross section of Specimen SL-1.9 (10X).

Figure 38. Optical micrograph of the microstructure near the sting on the cross section of Specimen SL-1.9 (100X).

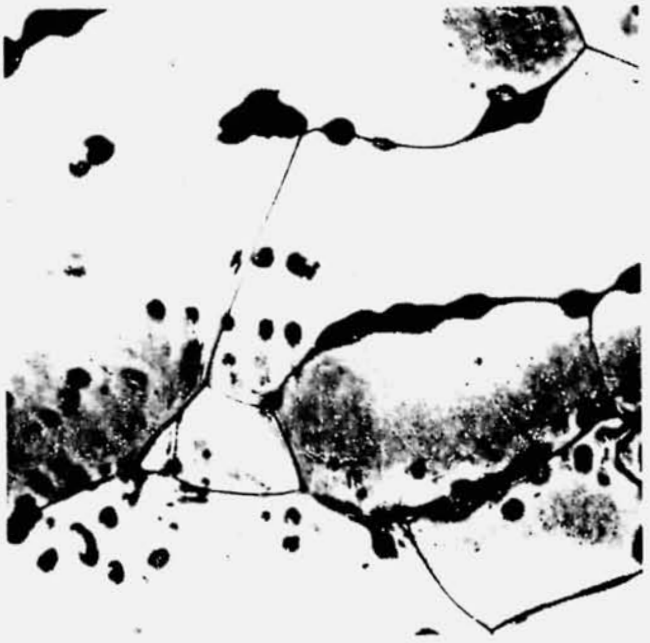

Figure 39. Optical micrograph of the microstructure near the protrusion boundary on the cross section of Specimen SL-1.9 (100X).

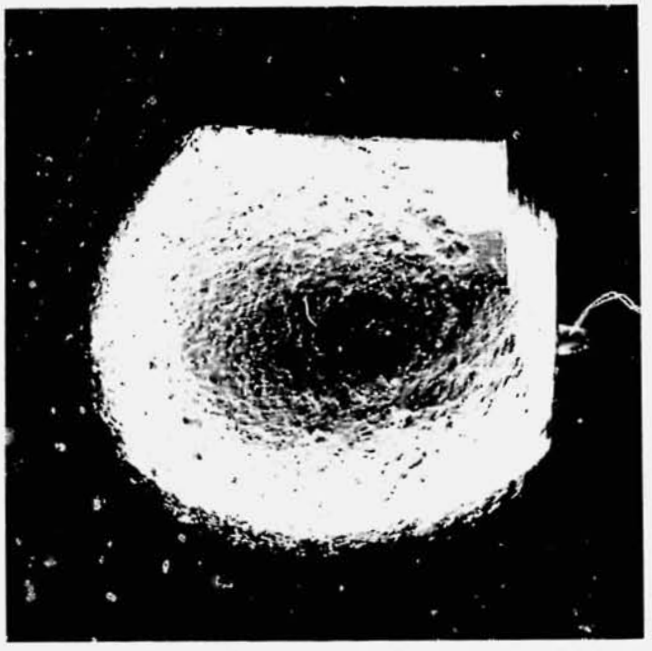

Figure 40. Profile view of Specimen SL-2.5 (10X).

Figure 41. Scanning electron micrograph of the resolidified surface of Specimen SL-2.5 near the sting side (250X).

Figure 42. Scanning electron micrograph of the resolidified surface of Specimen SL-2.5 near the top (100X).

Figure 43. Scanning electron micrograph of the top of Specimen SL-2.5 (25X).

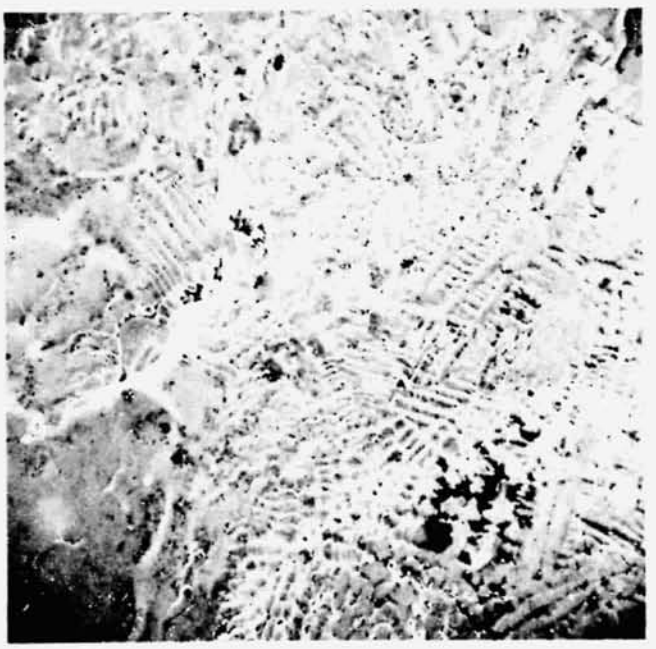

Figure 44. Scanning electron micrograph of an edge of the protrusion on Specimen SL-2.5 (100X).

Figure 45. Scanning electron micrograph of an edge of the protrusion on Specimen SL-2.5 (250X).

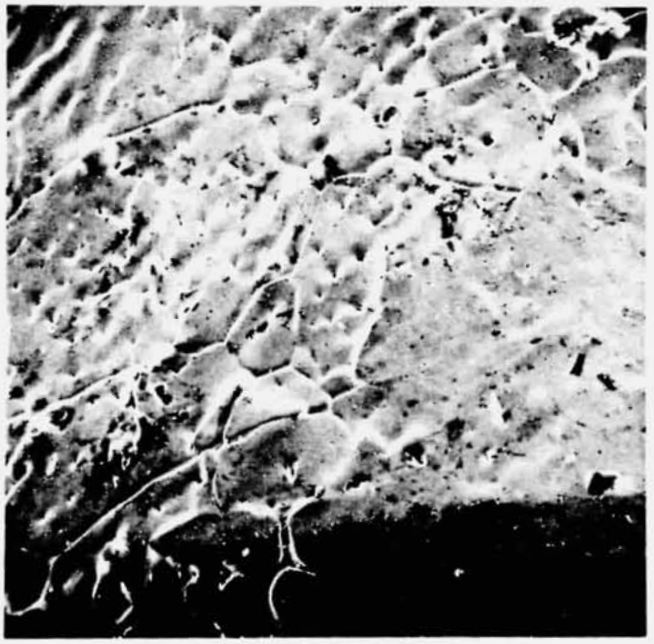

Figure 46. Scanning electron micrograph of the top surface of Specimen SL-2.5 at the resolidified - unmelted boundary (100X).

Figure 47. Scanning electron micrograph of the resolidified surface of Specimen SL-2.5 near the unmelted portion at the bottom of the specimen (250X).

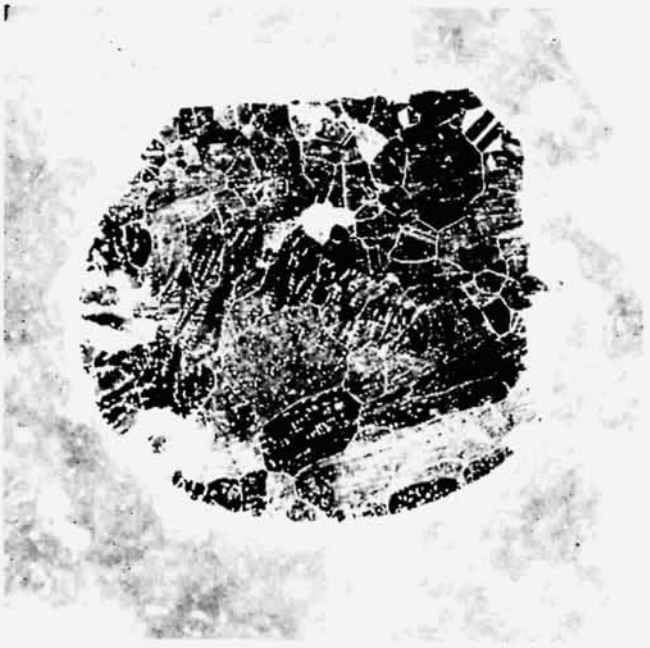

Figure 48. Optical macrograph of the polished and etched cross section of Specimen SL-2.5 (10X).

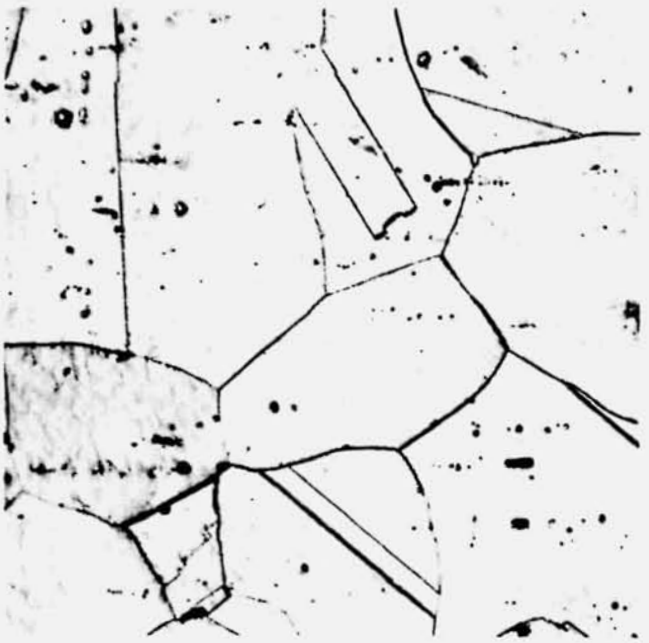

Figure 49. Optical micrograph of the etched cross section of Specimen SL-2.5 in the unmelted region (100X).

Figure 50. Optical micrograph of the etched cross section of Specimen SL-2.5 in the boundary between the resolifidied and unmelted portion (100X).

Figure 51. Optical micrograph of the etched cross section of Specimen SL-2.5 in the resolidified portion (100X).

☆U.S. GOVERMENT PRINTING OFFICE 1974 – 640-446 / 113 REGION NO. 4